Mild-temperature hydrodeoxygenation of vanillin a typical bio-oil model compound to creosol a potential future biofuel

Aliu, Elias; Hart, Abarasi; Wood, Joe

DOI:
10.1016/j.cattod.2020.05.066

Mild-Temperature Hydrodeoxygenation of Vanillin a typical Bio-Oil Model Compound to Creosol a Potential Future Biofuel.

Elias Aliu, Abarasi Hart, and Joseph Wood*

School of Chemical Engineering, University of Birmingham, Edgbaston, Birmingham B15 2TT, U.K.

*Corresponding Author: Tel: +44(0) 121 414 5295. Email: j.wood@bham.ac.uk

ABSTRACT

This study reports mild temperature hydrodeoxygenation (HDO) of vanillin an oxygenated phenolic compound found in bio-oil to creosol. It investigates the sensitivity of vanillin HDO reaction to changes in solvent, catalyst support and active metal type, and processing parameters using 100mL batch reactor. The processing parameters considered include temperature (318K – 338K), hydrogen gas pressure (1MPa – 3 MPa), catalyst loading (0.1kg/m^3 – 0.5kg/m^3), and agitation speed (500rpm-900 rpm). As expected, significant variation in conversion and product selectivity was displayed in the results. Among the solvents considered, 2-propanol and ethyl acetate produced the best performance with conversion close to 100% and selectivity toward creosol above 90%. Remarkable differences were found in the H_2 uptake during VL HDO reaction under different catalyst. The hierarchy in H_2 uptake of the catalysts include: Pd/C > PdRh/Al_2O_3 > Pd/Al_2O_3 = Pt/C > Pt/SiO_2 >> Rh/Al_2O_3. This was correlated to catalytic performance; Pd/C emerged as the best among the monometallic catalysts with 71 % selectivity toward creosol, but consumed 9 mmol of hydrogen per mol of vanillin converted. While the prepared bimetallic PdRh/Al_2O_3 catalyst consumed slightly lower amount of hydrogen (8 mmol), and produced significantly higher selectivity toward creosol (99%). Even after three cycles the prepared catalyst demonstrated superior performance over the monometallic catalysts with selectivity toward creosol above 80%. The reaction condition that maximises the degree of deoxygenation to creosol derived via Taguchi analysis includes temperature 338K, hydrogen gas partial pressure 3.0MPa, catalyst loading 0.5kg/m^3, and agitation speed 500rpm.

Keywords: Bio-oil; Vanillin; Creosol; Hydrodeoxygenation; Taguchi

1. Introduction

Fossil-derived fuels such as petroleum, coal and natural gas have long been the major source of energy to the world [1]. However, the capacity of light crude oil reserves responsible for producing most hydrocarbon fuels have been declining for many years. In addition, consumption of fossil derived fuels adversely affects the environment. As a result of these factors, attention has shifted toward alternative sources of energy. Preferably sources that are renewable and sustainable should be exploited [2–5]. Plant biomass represents a promising source of energy because of the renewability and reduced carbon footprint [6]. Liquid fuel known as bio-oil is usually produced from plant biomass via fast pyrolysis (FP), this process occurs rapidly (typically 1 - 2s) at temperatures around 773K in the absence of air [7–11]. As a result, produced bio-oil usually contains a significant amount of thermodynamically unstable oxygenated compounds [12–15]. Up to 400 different oxygenated compounds have been reported in analytical studies on bio-oil [16–18]. In contrast, the oxygen content in conventional fuels is less than 1 wt %. This high oxygen content in bio-oils (20-30 wt %) leads to problems such as blocked filters, excessive corrosion, pump breakdown etc. during initial attempts to substitute conventional fuels with bio-oils in operation of furnaces, gas turbines, boilers and space heaters [19–23]. Hence, upgrading is necessary for bio-oils to fulfil their potential as substitute fuels. Hydrodeoxygenation (HDO) is the leading technology for upgrading them. It involves rejection of oxygen from the bio-oil with hydrogen as the reducing agent, and usually involves temperatures of 423 to 573K and 7.5 to 30 MPa hydrogen gas pressure. However, the complexity of bio-oil and HDO reaction network compelled many laboratory scale studies to single or mixtures of model compounds present in bio-oil [24–28]. Common model compounds used in past studies on HDO include cresol, guaiacol, and anisole. These compounds were chosen because they contain multiple functional groups and are member of the guaiacyl species [29]. These species are favoured as model of oxygenates in bio-oil because they represent the primary structure of lignin fraction used to produce bio-oil. Vanillin (VL), an aromatic aldehyde compound cited in different analytical studies on bio-oil, is of interest in this work. This compound is selected because it contains a carbonyl group

which is largely responsible for the thermodynamic instability of real bio-oil [30–34]. Moreover, the three functional groups aldehyde, ether, and hydroxyl present in the structure of vanillin makes it a good representative model of oxygenates present in bio-oil. Finally, it belongs to the same group as cresol, guaiacol, and anisole. Catalysts used in past studies on real bio-oil and model compound HDO reactions include transition sulfided metals (CoMoS, and NiMoS), noble or precious metals (Pd, Pt, Ru and Rh) and non-noble metals (Ni, Cu, Fe, and their alloys) [28,35]. Looking at the performance of these catalysts in past HDO studies, undoubtedly noble metals demonstrated superior activity. However, the exorbitant cost in procuring these metals and ease at which they are poisoned raises concerns about the economics of the process [36–38]. Fortunately, resistance of these metals to poison can be increased by combining them with another metal. In addition, higher selectivity toward deoxygenated products was achieved in past HDO studies that utilised bimetallic catalysts [39–41]. Hence, a novel bimetallic catalyst comprising of palladium and rhodium on alumina support was synthesised, characterised and tested in this work. Furthermore, the catalytic performance of noble metals (Pd, Rh and Pt) on inert (c) and conventional supports (SiO_2 and Al_2O_3) were compared to the synthesised bimetallic catalyst. The role of solvent and processing parameters in VL HDO reaction was probed using different solvents and conditions. Finally, Taguchi analysis was used to derive the best mild condition for transforming vanillin to creosol which is a potential future biofuel.

2. Experimental

2.1. Synthesis of $PdRh/Al_2O_3$ catalyst

$PdCl_2$ solution (10.0g, 5 wt % in 10 wt % HCl, Sigma – Aldrich) was added dropwise to methanol (30 ml, Fischer Scientific, 99%) under vigorous stirring and then 5wt % Rh/Al_2O_3 (10.0g, Johnson Matthey) was introduced. The resultant mixture was stirred at room temperature for 4h and dried overnight at 298K. Further drying in an oven set at 353K was carried out for 2h prior to calcination at 773K for 4h.

2.2. Characterisation of the Catalysts

Nitrogen adsorption – desorption isotherms of the catalyst used in this study were obtained from Micromeritics Analytical Instrument ASAP 2010. The Brunauer- Emmett- Teller (BET) method was used to determine surface area of the catalysts, while Barrett-Joyner-Halenda (BJH) method was used to characterise pore size distribution. The outgassing conditions employed were: alumina supported catalysts (523K for 4h), Pt/C (373K for 4h), Pd/C (623K for 12h), and Pt/S (393K for 2h). The surface morphologies of spent and raw catalysts were examined using HITACHI TM3030 Plus Tabletop Scanning Electron Microscopy (SEM). In addition, crystallinity of the catalysts were probed using D8 Advanced X-Ray Diffraction (XRD) with a Cu-Kα radiation source (λ = 1.54056 Å) operated at 40 kV and 200mA. The speed of scanning was 3°/min over a range of 5° to 70°.

2.3. Experiments

In this work, all the experiments were carried out in a 100mL stainless steel batch reactor supplied by Parr Instruments. The model of the autoclave is 4848, it has a maximum permissible operating temperature of 648K. While the maximum permissible operating pressure is 10MPa. A comprehensive description of the reactor system has been reported in previous work by Aliu et al. [27].

2.3.1. Solvent Testing

VL HDO reaction was carried out in six different solvents, this includes water, ethylacetate, cyclohexane, tetrahydrofuran, 2-propanol, and toluene. In a standard experiment, the autoclave was charged with 0.055 dm^3 of the solvent, 0.385g fresh $PdRh/Al_2O_3$ catalyst and 2.20g vanillin (Sigma-Aldrich, 99%). It is important to note that the vanillin completely dissolved in all solvents tested in the study. The autoclave was sealed and flushed with N_2 gas three times to create an inert atmosphere. Subsequently, the autoclave was heated under constant stirring speed of 150 rpm to the reaction temperature of 318K. H_2 gas was then added to achieve desired reaction pressure of 5.6MPa and stirring speed increased from 150 to 1000 rpm. The length of each reaction was 0.5h, and the resultant mixture was filtered prior to analysis on a gas chromatography unit equipped with flame ionization detector (GC-FID).

2.3.2. Catalyst Testing

VL HDO reaction was conducted with six different catalysts, this includes 5 wt % Pd/C (Alfar Aesar), 5 wt % Pt/C (Sigma- Aldrich), 5 wt % Pd/Al_2O_3 (Johnson- Matthey), 5 wt % Rh/ Al_2O_3 (Johnson-Matthey), 5 wt % Pt/SiO_2 (Johnson-Matthey) and 6.5 wt % $PdRh/Al_2O_3$ (synthesised). Apart from $PdRh/Al_2O_3$ catalyst synthesised by modifying Rh/Al_2O_3, the other catalysts samples are commercially obtained. In a standard experiment, the autoclave was loaded with 0.075 dm^3 ethyl acetate, 0.5g of fresh catalyst and 2940mg vanillin (Sigma-Aldrich, 99%). However, 0.385g of the synthesised catalyst was used in the experiment to offset the difference in metal loading. These reactions were carried out at 338K, 2.0 MPa, 1000 rpm and 1h using the procedure described in Section 2.3.1. To discern the role of support and thermal effect on VL HDO reaction, additional experiments were carried out with no catalyst, 0.25g activated carbon (C), 0.25g silica (SiO_2), and alumina (Al_2O_3) at the same condition used to test all the catalysts. Stability of the catalysts were examined over three cycles, no special treatment was applied to the catalyst before reuse. At the end of each cycle, the catalyst was recovered from the reactor solution through filtering. Subsequently, they were dried at room condition overnight before reuse.

2.3.3. Effect of Processing Parameters

VL HDO reaction was carried out under 9 different conditions using 10 wt % Pd/C catalyst (Alfar Aesar) to determine the best combination of processing parameters that optimises conversion and degree of VL deoxygenation to creosol. The Taguchi method of experimental design [42,43] was used to establish these conditions (Table 1), a typical range of values found in the literature for each parameter were used to construct the matrix of experimental test conditions. This includes temperature 318 – 338K, pressure 1 – 3 MPa, catalyst loading 0.1 – 0.5 kg/m^3, solvent ethyl acetate and agitation speed 500 – 900 rpm (see Table 2). The procedure described in Section 2.3.1 was used to conduct all the experiments. VL conversion (X_{VL}), selectivity to vanillyl alcohol (S_{VA}), selectivity to creosol (S_{CR}), degree of deoxygenation (DOD) defined as the conversion of vanillin to creosol, which involves the removal of one oxygen atom, degree of hydrogenation (HYD) based on vanillin conversion to vanillyl alcohol,

and the relative rate of deoxygenation to hydrogenation (DOD/HYD) were determined through the following equations:

$$X_{VL}\ (\%)\ = \frac{C_{VL0} - C_{VL}}{C_{VL0}} \times 100 \quad (1)$$

$$S_{VA}\ (\%)\ = \frac{C_{VA}}{\sum C_i} \times 100 \quad (2)$$

$$S_{CR}\ (\%)\ = \frac{C_{CR}}{\sum C_i} \times 100 \quad (3)$$

$$DOD\ (\%)\ = \frac{C_{CR}}{C_{VL0}} \times 100 \quad (4)$$

$$HYD(\%) = \frac{C_{VA}}{C_{VL0}} \times 100 \quad (5)$$

$$\frac{DOD}{HYD}(\%)\ = \frac{C_{CR}}{C_{VA}} \times 100 \quad (6)$$

where C_{VL0} is initial VL concentration, C_{VL} is final VL concentration, C_{VA} is vanillyl alcohol concentration, and C_{CR} is creosol concentration.

2.4. Quantification of Reactant and Products

The samples collected from experiments were analysed via an automated trace gas chromatograph with flame ionisation detector (GC- FID) containing a ZB-Wax column (specification: 250 µm × 0.25 µm × 30m). A ramp of 10 K/min was applied to increase the column temperature from 313K to 513K, this final temperature was maintained for additional 5mins. Prior analyses were carried out using a mass spectrometer to identify specific components within the samples. Calibration curves developed from response of the components was used to determine composition of the reaction samples.

3. Results and Discussion

The range of conditions investigated ensures liquid phase only reaction with insignificant coke and gas formation. Also, negligible changes in the weight of solvents used were observed, which suggests the solvents are not converted into gases. Consequently, only two products vanillyl alcohol and creosol were recorded, meaning the solvents were not involved in the reaction. This section is organized as

follows; characteristics of the catalysts used are presented and discussed in section 3.1, discussion on solvent effect in section 3.2, catalyst effect discussion in section 3.3 and effect of processing parameters in section 3.4.

3.1. Characterisation of catalysts

The physicochemical properties of catalysts used in this work determined from N_2 adsorption-desorption isotherms are presented in Table 3. It shows that catalysts supported on carbon have higher surface areas compared to alumina and silica. However, Pt/SiO_2 has the largest pore volume and average pore diameter. Interestingly, impregnation of Pd into the commercial Rh/Al_2O_3 resulted in approximately 11% reduction in surface area and 8% decrease in pore volume. Furthermore, the average pore diameter of all the catalysts shown in Table 3 are greater than 2nm but less than 50nm. Hence, they are mesoporous materials and therefore exhibit type IV Isotherms. In addition, Table 3 shows that the particles of catalysts used in this work are less than 100µm in size. It has been shown that intraparticle mass transfer resistance is insignificant when the particle sizes are less than 250µm [27]. Hence, the discrepancies in the particle size has no influence on the reaction. Furthermore, most of the catalysts has average crystallite size less than or equal to 10nm. The only exception is Pt/SiO_2 catalyst with average crystallite size slightly higher than 10nm. The SEM-EDX images of unmodified Rh/Al_2O_3 and Pd-modified Rh/Al_2O_3 catalysts can be seen in Figure 1. It shows that the SEM micrograph of the precursor Rh/Al_2O_3 catalyst in Figure 1Aa differs from that of the synthesised $PdRh/Al_2O_3$ catalyst in Figure 1Ba. The latter appears to contain more agglomerated catalyst particles which suggest reduction in sizes of some of the catalyst particles post impregnation. As expected, the trace summarising the elemental composition of the precursor Rh/Al_2O_3 in Figure 1Ab contained one less peak compared to that of the synthesised bimetallic catalyst (See Figure 1Bb). The additional peak in the synthesised bimetallic catalyst trace affirms the introduction of Pd. Through XRF analysis, it was established that the added Pd co-existed with Rh in the synthesised $PdRh/Al_2O_3$ catalyst.

The XRD pattern of fresh and spent catalysts in Figure 2 shows that VL HDO reaction did not induce significant structural changes, in particular new phases were not formed. XRD pattern of Rh/Al_2O_3 shows distinct diffraction peaks which can be assigned to Al_2O_3 at $2\theta = 10°$, 46°, and 67°. In addition, a narrow diffraction peak attributable to Rh (311) can be seen at $2\theta = 86°$. Interestingly, the XRD pattern of the modified Pd catalyst is the same as the unmodified Rh/Al_2O_3 because characteristic diffraction peaks of Pd overlap with those of Al_2O_3.

3.2. Solvent Effect

In order to understand the role of solvent in VL HDO reaction, the distribution of products and conversion from the reaction in six different solvents were examined. These solvents can be put into three classes based on values of their dielectric constant (ε), dipole moment (μ), and hydrogen bond donor (HBD) capability (α) displayed in Table 4. The classes include: 1) Polar Protic Solvents: Water and 2-propanol characterised with high polarity and HBD capability ($\alpha > 0.7$). 2) Aprotic polar solvents: ethyl acetate and tetrahydrofuran with attributes of high polarity and low HBD capability ($\alpha \approx 0$). 3) Aprotic apolar solvents: cyclohexane and toluene with no HBD capability and extremely low ε and μ. The results are presented in Figure 3, both VL conversion and product distribution were significantly affected by changes in the reaction solvent. This observation is consistent with previous reports on dramatic effect of solvent on low temperature hydrogenation reactions [44–46]. In terms of conversion, solvent effectiveness follows the order: 2-Propanol > Ethyl Acetate > Tetrahydrofuran > Cyclohexane > Water > Toluene. Based on selectivity to the desired deoxygenated product creosol, the ascending order of solvent effectiveness is 2-Propanol > Ethyl Acetate > Cyclohexane > Tetrahydrofuran > Water > Toluene. From Figure 3, it can be seen that close to 100% conversion was achieved under 2-propanol and ethyl acetate. Likewise, selectivity toward the desired deoxygenated product creosol was above 90% under these solvents. Hence, both 2-propanol and ethyl acetate are the most effective among the various solvents used in this study. From stoichiometry of the reaction,

19.7mmol of vanillin requires approximately 39.5mmol of hydrogen gas for full conversion and 100% selectivity toward creosol the desired product. However, it was found that to convert 1mol of vanillin, 4mmol of H_2 is required in cyclohexane, 6mmol of H_2 is needed in toluene, 8mmol of H_2 is needed in ethyl acetate, 9mmol of H_2 is required in tetrahydrofuran, 11mmol of H_2 is required in water and 13mmol of H_2 is needed in 2-propanol. This result indicates that vanillin easily hydrogenates under the various solvents. From the work of Wan.et.al [43], changes in solvent properties affected H_2 uptake and conversion, with the highest activity achieved in polar protic solvents and the lowest activity in aprotic polar solvents. In agreement, Figure 4 shows significant differences in the H_2 uptake (the drop in initial H_2 gas pressure was assumed to be representative of hydrogen consumed during the reaction) under the various reaction solvents considered. In contrast to findings in Wan et al [43], the synthesised bimetallic $PdRh/Al_2O_3$ catalyst performed better in aprotic polar solvents than aprotic apolar solvents. The percentage decrease relative to the initial H_2 gas pressure of 5.6 MPa was 35.7% in 2-propanol, 5.4% in water, 28.6% in ethyl acetate, 25.0% in tetrahydrofuran, 16.1% in toluene and 14.6% in cyclohexane. It is apparent that solvents within the same class and dielectric constant (see Table 4) exhibit similar H_2 uptake. The initial turn over frequency (TOF) of $PdRh/Al_2O_3$ catalyst in different solvents was estimated using the method described in Wan.et.al [43]. From the polynomial fit to the experimental H_2 uptake profiles, the initial hydrogenation rates were estimated numerically by finding the slope at t=0mins. Subsequently, the catalyst molecular weight (M_{cat}), metal dispersion (D) and estimated initial hydrogenation rates (r_H) were substituted into equation 7 to determine the equivalent initial TOF of the catalyst in different solvents.

$$\mathrm{TOF} = \left(\frac{\mathrm{r_H\ M_{cat}}}{\mathrm{D}}\right) \qquad (7)$$

Notably, the trend in estimated initial TOF values follows the same pattern observed from analysing the H_2 uptake. Although the adsorption of polar reactant such as vanillin is more favourable in non-polar solvents such as toluene and cyclohexane [46], reduced catalytic activity were observed in these solvents because of the low H_2 uptake. Remarkably low initial TOF was estimated for the catalyst in

the presence of water as the reaction solvent, this could be attributed to the unfavourable adsorption of vanillin and remarkably low H_2 uptake (see Figure 4). In general, Table 4 shows an inverse relationship between the measured initial TOF of the prepared $PdRh/Al_2O_3$ catalyst, and the dielectric constant for solvents in the same class. Likewise, for solvents in the same class the measured initial TOF is higher in the solvent with lower hydrogen bond acceptor. The only exception is water in which the measured initial TOF is remarkably smaller than that measured in 2-propanol. This could be as a result of the significantly higher hydrogen bond donor capability of water compared to 2-propanol.

3.3. Catalyst Effect

In order to examine the influence of support on VL HDO reaction, the reaction was conducted using activated carbon (C), alumina (Al_2O_3), and silica (SiO_2) as described in Section 2.3.2. The results are presented in Table 5, it clearly indicates negligible contribution from catalytic supports with no more than 4% conversion achieved. This is consistent with previous work on VL HDO reaction kinetics on 10 wt % palladium on activated carbon [27]. Conversely, Figure 5 shows that changes in the catalyst active metal significantly affected conversion and product selectivity. These changes can be attributed to variation in the metal dispersion, metal grain size and metal-support interaction because contribution from non-catalytic reaction and catalytic supports are not significant in VL HDO reaction (see Table 5). In addition, Figure 6 shows remarkable variation in the H_2 uptake during VL HDO reaction in the presence of different catalysts using ethyl acetate as the solvent. The percentage decrease relative to the initial H_2 gas pressure of 5.6 MPa was 30.4% for Pd/C, 28.6% for $PdRh/Al_2O_3$, 5.4% for Rh/Al_2O_3, 13.0% for Pt/SiO_2, and 17.9% for both Pd/Al_2O_3 and Pt/C. Under different catalysts, the number of moles of hydrogen required to convert 1mol of vanillin found was 9mmol using Pd/C, 8mmol using $PdRh/Al_2O_3$, 6mmol using either Pt/C or Pt/SiO_2, and 5mmol using either Pd/Al_2O_3 or Rh/Al_2O_3. Based on the presented information, Rh/Al_2O_3 and Pd/Al_2O_3 are the most attractive among the tested catalysts from a commercial point of view because both requires the least amount of hydrogen. However, Figure 5 shows that remarkably low conversion and selectivity toward creosol was achieved

using Rh/Al_2O_3 catalyst. In terms of conversion, performance of the catalysts can be ranked in the order: Pd/Al_2O_3 > Pd/C > $PdRh/Al_2O_3$ >> Pt/C > Pt/SiO_2 >> Rh/Al_2O_3. On the other hand, performance in terms of selectivity toward the desired product creosol follows this order: $PdRh/Al_2O_3$ >> Pd/C >> Rh/Al_2O_3 >> Pt/SiO_2 > Pd/Al_2O_3 > Pt/C. Notably, high conversion was achieved using Pd-based catalysts while Rh/Al_2O_3 catalyst with the least H_2 uptake and conversion showed good selectivity toward creosol. Hence, it was necessary to test the combined effect of Pd and Rh. Indeed, the prepared bimetallic $PdRh/Al_2O_3$ catalyst demonstrated better performance over the monometallic catalysts (see Figure 5). Among the monometallic catalysts, Pd/C consumed the highest amount of hydrogen and produced the highest selectivity toward creosol of 71%. However, the prepared bimetallic $PdRh/Al_2O_3$ consumed less hydrogen and produced 99% selectivity toward creosol. This represents 28% gain in selectivity toward the desired deoxygenated product. It is worth highlighting that the observed remarkable difference between the H_2 uptake in the presence of Pd/C and $PdRh/Al_2O_3$ could be associated to the former having smaller particle size, much bigger metal dispersion and surface area (see Table 3).

The result of an additional test carried out to examine stability of all the catalysts can be seen in Table 6. It clearly showed negligible changes in conversion achieved over three cycles using Pd/C and Pt/C. Whereas, the conversion achieved using Pd/Al_2O_3 decreased marginally by 2% over the three cycles. Interestingly, conversion increased by about 22% over the three cycles in the presence of Rh/Al_2O_3. A plausible reason for this strange behaviour is reduction in rhodium oxide to active metallic rhodium following prolong exposure to hydrogen. However, this observation is consistent with the low H_2 uptake under Rh/Al_2O_3 shown in Figure 6. As a result, Rh/Al_2O_3 requires longer time to achieve full active state compared to Pd/C with higher H_2 uptake. Notably, Pt/SiO_2 with slightly better H_2 uptake than Rh/Al_2O_3 showed 23% increase in conversion between the first and second cycle. But the conversion decreased by 14% from second to third cycle. This is due to reduction from platinum oxides to active platinum metal followed by slight deactivation between the second and third cycles. The improved H_2 uptake of Pt/SiO_2 clearly help reduced the length of time for activation in comparison to

Rh/Al_2O_3. After three cycles, the order in performance of the catalysts based on selectivity toward creosol includes $PdRh/Al_2O_3$ > Pd/C >> Rh/Al_2O_3 >> Pd/Al_2O_3 > Pt/C >> Pt/SiO_2. However, one of the drawbacks of carbon supported catalyst is the challenge of regeneration particularly deactivation due to carbon deposit. Interestingly, the use of bimetallic $PdRh/Al_2O_3$ catalyst further increased the selectivity toward creosol by 27.8%. This increase can be attributed to the synergy between Pd and Rh. In addition, the synthesised bimetallic catalyst demonstrated excellent stability, with conversion close to 100% achieved after three cycles. It is worth mentioning that at elevated temperatures, coking largely responsible for deactivation is more likely [26, 36]. The slight drop in conversion and creosol selectivity observed in some catalysts such as Pt/SiO_2 could be attributed to the reduced strength of active sites or minor leaching of active metal from the support materials after successive reaction or caused by the agitation speed, since no coke formation was recorded. Hence, the mild temperatures used in this study accounts for the low deactivation witnessed in most of the catalysts.

3.4. Effect of Processing Parameters.

In order to understand the influence of processing parameters on key performance indicators (i.e. degree of deoxygenation, conversion, and ratio of deoxygenation to hydrogenation), VL HDO reactions were carried out under 9 different conditions using 10wt% Pd/C catalyst and ethyl acetate as solvent. The processing parameters considered in the study include temperature, catalyst loading, hydrogen gas partial pressure, and agitation speed.

Figure 7 summarises the conversion and product selectivity achieved in each of the experiments (see Tables 1 and 2). It shows that VL HDO reaction is sensitive to changes in the processing parameters, with both conversion and product selectivity changing with the reaction conditions.

Taguchi analysis was used to isolate the effect of changes in each of the processing parameters on the KPIs. It involves the use of appropriate signal to noise ratio (S/N) function. To determine the best configuration of processing parameters that ensures excellent KPIs, the larger is better approximation was used to compute the S/N ratio. It is worth mentioning that the derived configuration of processing

parameters is limited to the range considered in this work. Additional details on Taguchi analysis has been published elsewhere [50].

3.4.1. Effect of Temperature.

The range of temperature 318K-338K ensures the reaction remains in the liquid phase and minimise coke and gaseous products formation. Figure 8 summarises the influence of temperature on VL HDO reaction, it shows that conversion and degree of deoxygenation (DOD) increases as temperature increases from level 1 (318K) to level 3 (338K). Likewise, the selectivity toward creosol increases at the expense of vanillyl alcohol from level 1 to level 3. This observation reaffirms the well-known Arrhenius behaviour of increased reaction rates with temperature. In addition, it is consistent with findings from Mahfud et al [51]. Consequently, within the range of temperature considered in this study, 338K maximises VL conversion to creosol the product of interest.

3.4.2. Effect of Pressure.

The effect of changes in pressure on conversion, degree of deoxygenation and hydrogenation are presented in Figure 9. It shows that VL conversion was not significantly affected by changes in the reaction pressure from level 1 (1.0 MPa) to level 3 (3.0MPa). However, remarkable changes can be seen in the degree of deoxygenation and hydrogenation as reaction pressure increases from 1.0 to 3.0 MPa. This observation is in agreement with claim in literature that higher reaction pressure favours deoxygenation of vanillyl alcohol to creosol [37]. Besides, at high reaction pressure more hydrogen atoms are available to react with VL. Based on the observed trend, it can be concluded that within the range considered in this study, 3.0 MPa is the most suitable hydrogen gas partial pressure for VL HDO reaction.

3.4.3. Effect of Catalyst Loading.

The impact of changes in catalyst loading from level 1 (0.5 kg/m^3) to level 3 (0.1 kg/m^3) on conversion, degree of deoxygenation and hydrogenation are presented in Figure 10. It can be seen that degree of

deoxygenation and conversion increased as the catalyst loading increases from 0.1 to 0.5 kg/m^3. A plausible reason for the observed trend is increase in the number of available active sites following increase in the catalyst loading. As a result of this change, the number of active sites accessible to the reactants increases. Likewise, the reactants converted increases and the degree of deoxygenation improves. Therefore, in the range considered 0.5 kg/m^3 is the most appropriate catalyst loading.

3.4.4. Effect of Agitation Speed.

The influence of agitation speed on conversion, degree of deoxygenation and hydrogenation can be seen in Figure 11. It clearly shows that all three parameters were insensitive to agitation speed over the range considered; 500 (level 1) to 900 rpm (level 3), and thereby indicates absence of external mass transfer limitation in the system [52]. As a result, 500 rpm is considered the optimum speed since higher agitation rate is at the expense of energy cost.

3.4.5. Analysis of Variance (ANOVA).

To prioritize the importance of the different processing parameters on the degree of deoxygenation, analysis of variance (ANOVA) was carried out following the procedure described in literature [42]. The matrix of input data showing the degree of deoxygenation at the various conditions is presented in Table 7. These data were used to determine the signal to noise ratio, total sum of squares deviation, mean variance, and percentage contribution (P). In addition, the degrees of freedom (DOF) for the parameters were calculated by subtracting 1 from the number of levels considered. The results obtained are presented in Table 8. From these statistics, it can be concluded that the parameters considered completely explained changes in the degree of deoxygenation achieved. For instance, changes in the catalyst loading accounts for 77.2% of the variation in the degree of deoxygenation achieved. While, changes in the agitation speed accounts for 0.1% of the variation in the degree of deoxygenation achieved. The order of influence of the parameters on the degree of deoxygenation achieved is as follows: catalyst loadings >> reaction temperature >> reaction pressure >> agitation

speed. Hence, catalyst loading has the most significant effect on the degree of deoxygenation achieved from the reaction.

4. Conclusion

In this work, vanillin (VL) a model compound of bio-oil was used to investigate the effect of solvent, catalyst active metal, supports and processing parameters on hydrodeoxygenation (HDO) reaction. It was observed that non-catalytic and catalytic support influences on the reaction are not significant when compared to the catalytic active metals (Pd, Pt, Rh, and PdRh). Product distribution and conversion changed significantly with the reaction solvents. This was correlated to observed differences in percentage decrease in the initial H_2 gas pressure under various solvents. The highest decrease of 35.7% was obtained under 2-propanol while in the presence of water the lowest drop of 5.4% was achieved. This means hydrogen is more soluble in 2-propanol than water. However, approximately the same amount of hydrogen is needed to attain the same level of conversion in both solvents. Interestingly, H_2 uptake and initial turn over frequency for solvents with similar dielectric constant are almost the same. Among the solvents tested, 2-propanol and ethyl acetate showed the most promising performances with conversion and selectivity toward creosol close to 100%. In addition, the result of reactions conducted under different catalyst active metals showed remarkable variation in product distribution, conversion, and H_2 uptake. Among the investigated active metals, the highest conversion of 99% was achieved using Pd based catalysts followed by Pt catalysts and then Rh based catalyst. The observed pattern is consistent with the uptake of H_2, the highest percentage decrease in initial H_2 gas pressure of 30.4% was achieved in the presence of Pd/C and the lowest value of 5.4% was obtained using Rh/Al_2O_3. Additionally, the stability and reusability tests conducted showed insignificant deactivation in most of the catalysts after three cycles. Among the monometallic catalysts, Pd/C was the most stable with conversion close to 100% after three cycles. Conversely, Pt/SiO_2 proved to be the least stable with remarkable drop of 13.5 % in conversion between the second and third cycle. Notably, the synthesised $PdRh/Al_2O_3$ catalyst demonstrated excellent stability

and performance over the best monometallic catalyst (Pd/C) with conversion close to 100% and 83% selectivity toward creosol after three cycles. Finally, Taguchi analysis was successfully used to derive the condition which maximises the degree of deoxygenation to creosol from f VL HDO reaction. The derived condition includes: temperature 338K, hydrogen gas partial pressure 3.0 MPa, catalyst loading 0.5 kg/m^3, and agitation speed 500 rpm.

Acknowledgements

The financial support for this work was provided by School of Chemical Engineering, University of Birmingham.

References

[1] Q .Lai, C . Zhang, J.H. Holles, Appl Catal A Gen 528 (2016) 1–13.

[2] M. Patel, A. Kumar, Renew Sustain Energy Rev 58 (2016) 1293–1307.

[3] M. Lu, H. Du, B. Wei , J. Zhu , M. Li , Y. Shan, Energy Fuels 31 (2017) 10858 - 10865.

[4] B.Raj, O.Singh, Foss Fuel Environ 8 (2012) 168 - 188.

[5] Y.Wang, T.He, K. Liu, J.Wu, Y.Fang, Bioresour Technol 108 (2012) 280–284.

[6] X.Zhang, J.Long, W.Kong, Q. Zhang, L .Chen, T.Wang, Energy Fuels 28 (2014) 2562–2570.

[7] Y.Solantausta, A.Oasmaa, K.Sipilä, C.Lindfors, J.Lehto, J.Autio, Energy Fuels 26(2012) 233–240.

[8] A.V. Bridgwater, Catal Today 29 (1996) 285–295.

[9] A.V. Bridgwater , Appl Catal A. Gen 116 (1994) 5–47.

[10] M.E. Boucher, A.Chaala, H. Pakdel, C.Roy, Biomass and Bioenergy 19 (2000) 351–361.

[11] A.V. Bridgwater, Biomass and Bioenergy 38 (2012) 68–94.

[12] S.Echeandia, B.Pawelec, V.L Barrio, P.L Arias, J.F Cambra, C.V. Loricera, Fuel 117 (2014) 1061–73.

[13] S.Boullosa-Eiras, R.Lødeng, H.Bergem, M.Stöcker, L.Hannevold, E.A Blekkan, Catal Today 223(2014) 44–53.

[14] J.Jae, G.A Tompsett, A.J Foster, K.D Hammond, S.M Auerbach, R.F Lobo, J Catal 279 (2011) 257–268.

[15] K . Li, R.Wang, J. Chen, Energy Fuels 25(2011) 854–863.

[16] T.P Vispute, G.W Huber, Green Chem 11(2009) 1433–1445.

[17] D. Klass, Biomass for Renewable energy, fuels and Chemicals, first ed., Academic Press, San Diego,1998.

[18] S.Czernik, A. V. Bridgwater, Energy Fuels 18(2004) 590–598.

[19] D.Mohan, C.U Pittman, P.H. Steele, Energy Fuels 20(2006) 848–889.

[20] L.Busetto, D.Fabbri, R.Mazzoni, M.Salmi, C.Torri, V. Zanotti, Fuel 90 (2011) 1197–1207.

[21] C.A Fisk, T.Morgan, Y.Ji, M.Crocker, C.Crofcheck, S.A Lewis, Appl Catal A Gen 358 (2009)150–156.

[22] J.P Diebold, A review of the chemical and physical mechanisms of the storage stability of fast pyrolysis bio-oils, National Renewable Energy Laboratory, 2000.

[23] E.Laurent, B.Delmon, Appl Catal A Gen 109 (1994) 77–96.

[24] Z.He, X.Wang, Catal Sustain Energy, 1 (2012) 28–52.

[25] L . Zhang, R.Liu, R.Yin, Y. Mei, Renew Sustain Energy Rev 24 (2013) 66–72.

[26] P.M Mortensen, J. D Grunwaldt, P.A Jensen, K.G Knudsen, A.D Jensen, Appl Catal A Gen 407(2011) 1–19.

[27] E. Aliu, A. Hart, J. Wood, Ind Eng Chem Res 58(2019) 15162 -15172.

[28] D.A Ruddy, J.A Schaidle, J.R Ferrell, J. Wang, L.Moens, J.E Hensley, Green Chem 16(2014) 454–490.

[29] W.Mu, H.Ben, A.Ragauskas, Y.Deng, Bioenergy Res 6(2013) 1183–1204.

[30] T.Hosoya, H.Kawamoto, S. Saka, J Anal Appl Pyrolysis 85(2009) 237 - 246.

[31] R.Lou, S. Wu Bin, L.v GJ. J Anal Appl Pyrolysis 89 (2010)191–196.

[32] R.Lou, S. Wu Bin, L.v GJ, D.L Guo. BioResources 5 (2010) 2184–2194.

[33] C.A Mullen, A.A Boateng. Fuel Process Technol 91 (2010) 1446–1458.

[34] Q. Yang, S. Wu, R. Lou, G. L.v, J Anal Appl Pyrolysis 87(2010)65-69.

[35] H.Wang, J.Male, Y. Wang, ACS Catal 3(2013)1047–1070.

[36] S.Cheng, L.Wei, X.Zhao, J. Julson, Catalysts 6(2016)195.

[37] L .He, Y .Qin, H.Lou, P. Chen, RSC Adv 5(2015) 43141–43147.

[38] R.Nie, H.Yang, H.Zhang, X.Yu, X.Lu, D.Zhou, Green Chem 19(2017) 3126–3134.

[39] D.C. Elliott, Curr Opin Chem Eng 9(2015) 59–65.

[40] A.R Ardiyanti, S.A Khromova, R.H Venderbosch, V.A Yakovlev, I .V. Melián-Cabrera, H.J Heeres, Appl Catal A Gen 449(2012) 121–130.

[41] C.C Schmitt,A.Zimina, Y.Fam,Catalysts 9(2019) 1-28

[42] S.R Rao, G. Padmanabhan, Int J Eng Res 2(2012) 192–197.

[43] M. Kowalczyk, Adv Manuf Sci Technol 38(2014) 2.

[44] H. Wan, A. Vitter, R. V. Chaudhari, B. Subramaniam, J Catal 309 (2014) 174-184.

[45] I . McManus, H. Daly, J.M Thompson, E. Connor, C.Hardacre, S.K Wilkinson, J Catal 330(2015) 344-353.

[46] J. He, C. Zhao, J.A Lercher. J Catal 309(2014) 362–375.

[47] B.S Akpa, C. D' agostino, L.F Gladden, K.Hindle, H.Manyar, J. Mcgregor, J Catal 289 (2012) 30 -41.

[48] E.M Kosower, J.Am. Chem. Soc 80 (1958) 3253

[49] M.H. Abraham, P.L. Grellier, J.L.M Abboud, R.M. Doherty. R.W. Taft, Can. J. Chem 66 (1988) 2673

[50] C. Reichardt, Chem.Rev 94 (1994) 2319.

[51] A. Al-Marshed, A. Hart, G. Leeke, M. Greaves, J. Wood, Energy Fuels 29 (2015) 6306 –6316.

[52] F.H Mahfud, F.Ghijsen, H.J Heeres, J Mol Catal A Chem 264(2007) 227–236.

[53] C.Perego, Catal Today 52(2002) 133–145.

Table 1. Constructed Orthogonal Array to Maximise Creosol Formation from Vanillin HDO Reactions

Run	T(K)	P(MPa)	CL(Kgm^{-3})	Agitation Speed(RPM)
1	318	1	0.5	500
2	318	2	0.3	700
3	318	3	0.1	900
4	328	1	0.3	900
5	328	2	0.1	500
6	328	3	0.5	700
7	338	1	0.1	700
8	338	2	0.5	900
9	338	3	0.3	500

*** T represents reaction temperature, P represents reaction pressure, CL represents catalyst loading, and rpm represents revolutions per minute.**

Table 2. Selected Control Factors and Associated Value to Each Level

Control Factors	Control Factor Levels		
	Level 1	**Level 2**	**Level 3**
Reaction Temperature (K)	318	328	338
H_2 gas Pressure (MPa)	1	2	3
Catalyst Loading (kg m^{-3})	0.5	0.3	0.1
Agitation Speed (rpm)	500	700	900

Table 3. Physicochemical Properties of Catalysts.

Catalyst	S_{BET} (m^2g^{-1})	V (cm^3g^{-1})	d_{AVG} (nm)	D (%)	d_p (µm)	D_m (nm)
5 wt % Pd/C	835	0.337	2.7	28.1	0.65-26	10.0
5 wt % Pt/C	1344	0.370	2.3	n/a	0.40-10	6.69
5 wt % Pd/Al_2O_3	108	0.125	4.9	n/a	0.60-81	8.14
5 wt % Rh/Al_2O_3	164	0.296	7.5	n/a	0.50-36	5.74
6.5 wt % $PdRh/Al_2O_3$	146	0.272	7.6	12.1	0.23-35	6.37
5 wt % Pt/SiO_2	272	0.717	11.4	n/a	1.10-84	10.2

- S_{BET} represents measured surface area of the catalysts, V represents the total specific pore volume of the catalysts, d_{AVG} represents the average pore size of the catalysts, D represents the metal dispersion estimated from CO chemisorption, d_p represents the range of particle size estimated from SEM micrographs using image J software, and D_m represents the average metal crystallite size estimated from XRD data.

Table 4. Parameters for different solvent [47 - 49]

Solvent	ε	μ	π*	$E_T(30)$	Z	α	β	TOF (min^{-1})
Water	78.5	1.85	1.09	63.1	94.6	1.17	0.47	1.3
2-Propanol	20.1	1.68	0.48	50.7	78.3	0.76	0.95	31.7
Ethylacetate	6.0	1.88	0.55	38.1	64.0	0.00	0.45	25.9
Tetrahydrofuran	7.6	1.63	0.58	37.4	58.8	0.00	0.55	19.3
Toluene	2.4	0.39	0.54	33.9	N/A	0.00	0.11	11.0
Cyclohexane	2.0	0.00	0.00	30.9	60.1	0.00	0.00	13.7

* ε represents dielectric constant, μ represents dipole moment, α represents hydrogen bond donor capability, β represents hydrogen bond acceptor capability, π* represents solvent dipolarity, TOF represents turn over frequency of the catalyst, $E_T(30)$ represents the Dimroth-Reichardt polarity scale, Z represents the scale of solvent ionizing power, and N/A means not available.

Table 5. Preliminary experiments to evaluate catalytic supports and non-catalytic effect on VL HDO reaction.

* Reaction Conditions: Feed vanillin concentration of 263mM, Temperature 338K, Hydrogen gas Pressure 2.0MPa, Agitation speed 1000rpm, catalytic support 0.25g, and batch time 1h.

Experiments	Initial Concentration (mM)	Final Concentration (mM)	Conversion (%)
No Catalyst	255.07	254.62	0.18
Activated Carbon (C)	254.12	244.63	3.73
Alumina (Al_2O_3)	258.58	255.95	1.02
Silica (SiO_2)	257.38	255.42	0.76

Table 6. Summary of Reusability and Stability Studies.

Catalysts	Conversion			Vanillyl Alcohol Selectivity			Creosol Selectivity		
	1	2	3	1	2	3	1	2	3
Pd/C	98.5	99.5	99.9	28.6	27.7	24.3	71.4	72.2	75.6
Pd/Al_2O_3	99.0	97.9	97.1	95.6	96.0	93.0	4.3	3.9	7.0
Rh/Al_2O_3	21.1	34.8	43.6	76.1	86.5	76.3	15.3	9.5	19.6
$PdRh/Al_2O_3$	97.8	98.9	99.9	0.8	14.3	17.0	99.2	85.3	82.7
Pt/C	41.9	39.4	45.0	96.6	83.5	92.9	1.9	15.6	6.3
Pt/SiO_2	36.6	59.5	46.0	92.4	96.7	98.2	7.2	3.3	1.7

* Reaction Conditions: Feed Vanillin Concentration 263mM, Temperature 338K, Hydrogen gas pressure 2.0MPa, Agitation Speed: 1000rpm, batch time 1h, $PdRh/Al_2O_3$ catalyst 0.385g, other catalysts 0.5g.

Table 7. Input Matrix for Analysis of Variance.

Matrix of Input Data For ANOVA							
Run	T(K)	P(bar)	CL(Kgm-3)	Agitation Speed(RPM)	DOD	S/N	(n-m)^2
1	318	10	0.5	500	14.77794	23.39228	7.5688459
2	318	20	0.3	700	7.528932	17.53467	9.6500691
3	318	30	0.1	900	6.548226	16.32247	18.650744
4	328	10	0.3	900	8.282689	18.36343	5.1878995
5	328	20	0.1	500	5.759799	15.20815	29.517239
6	328	30	0.5	700	19.64801	25.86637	27.303232
7	338	10	0.1	700	8.121298	18.19251	5.9957149
8	338	20	0.5	900	22.37536	26.9954	40.376845
9	338	30	0.3	500	15.6582	23.89484	10.586656
					Total	20.64112	154.83725

* T represents temperature, P represents hydrogen gas pressure, CL represents catalyst loading, rpm represents revolution per minute, DOD represents degree of deoxygenation, S/N represents the signal to noise ratio, n represents individual signal to noise ratio, and m is the mean signal to noise ratio.

Table 8. Analysis of variance result

Parameter	DOF	Sum of Squares	Mean variance	P (% cont.)	Rank
Temperature (K)	2	26.4	13.2	17.1	2
Pressure (bar)	2	8.7	4.3	5.6	3
Catalyst loading (kgm^{-3})	2	119.6	59.8	77.2	1
Agitator Speed (RPM)	2	0.2	0.1	0.1	4
Error	2	0	0	0	
Total	10	154.8	77.4	100.0	

* DOF means degree of freedom, and P represent the percentage contribution from each parameter.

List of Figure Captions

Fig. 1. SEM-EDX images of the (A) unmodified Rh/Al_2O_3 catalyst [(a) SEM micrograph, (b) EDX elemental composition, (c) Al mapping and (d) Rh mapping], and (B) Pd-modified Rh/Al_2O_3 catalyst[(a) SEM micrograph, (b) EDX elemental composition, (c) Pd mapping and (d) Rh mapping].

Fig. 2. XRD patterns of fresh and spent catalysts.

Fig. 3. Effect of solvent on VL HDO reaction and Product Distribution at initial hydrogen pressure 5.6 MPa, temperature 318K, feed VL concentration 263mM, stirring speed 1000 rpm, batch reaction time 0.5 h, and 0.385g $PdRh/Al_2O_3$.

Fig. 4. Temporal H_2 uptake profiles with 6.5 wt. % $PdRh/Al_2O_3$ catalyst at initial hydrogen pressure 5.6 MPa, temperature 318K, feed VL concentration 263mM, stirring speed 1000 rpm, batch reaction time 0.5 h, and 0.385g catalyst under different solvents.

Fig. 5. Influence of different catalyst on Conversion and Product Selectivity from VL HDO Reaction at hydrogen gas pressure 1.0 MPa, temperature 338K, feed VL concentration 263mM, stirring speed 1000 rpm, and batch reaction time 1h.

Fig. 6. Temporal H_2 uptake profiles with different catalysts at initial hydrogen pressure 5.6 MPa, temperature 318K, feed VL concentration 263mM, stirring speed 1000 rpm, batch reaction time 0.5 h, and ethyl acetate as the reaction solvent.

Fig. 7. Conversion and product distribution from VL HDO reaction under each of the experimental conditions in the designed L9 orthogonal array. [Note, BC: best condition].

Fig. 8. Main effect analysis of reaction temperature on conversion, degree of deoxygenation and hydrogenation using signal to noise ratio.

Fig. 9. Main effect analysis of reaction pressure on conversion, - degree of deoxygenation and hydrogenation using signal to noise ratio.

Fig. 10. Main effect analysis of catalyst loading on conversion, degree of deoxygenation and hydrogenation using signal to noise ratio.

Fig.11. Main effect analysis of agitation speed on conversion, degree of deoxygenation and hydrogenation using signal to noise ratio.

Figure 1

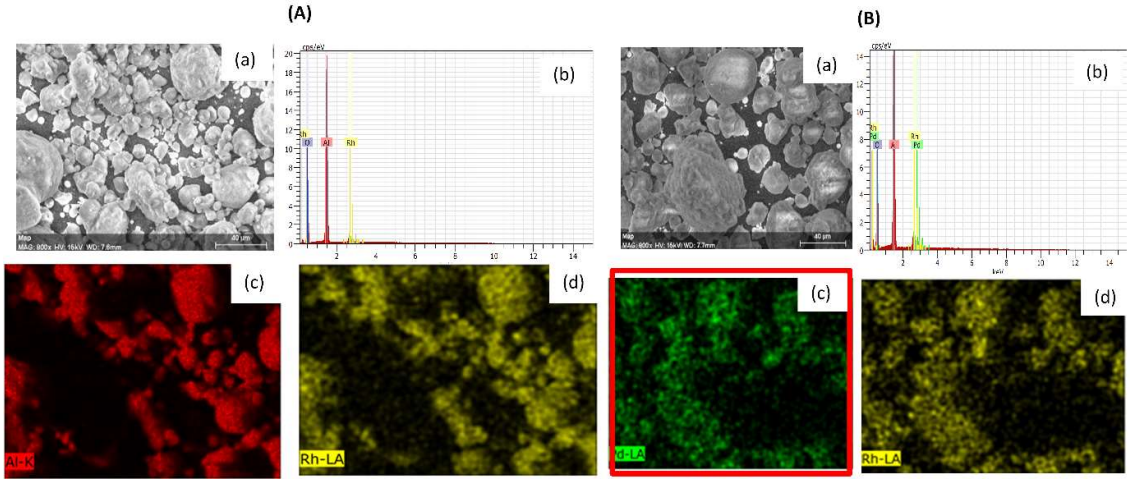

Figure 2

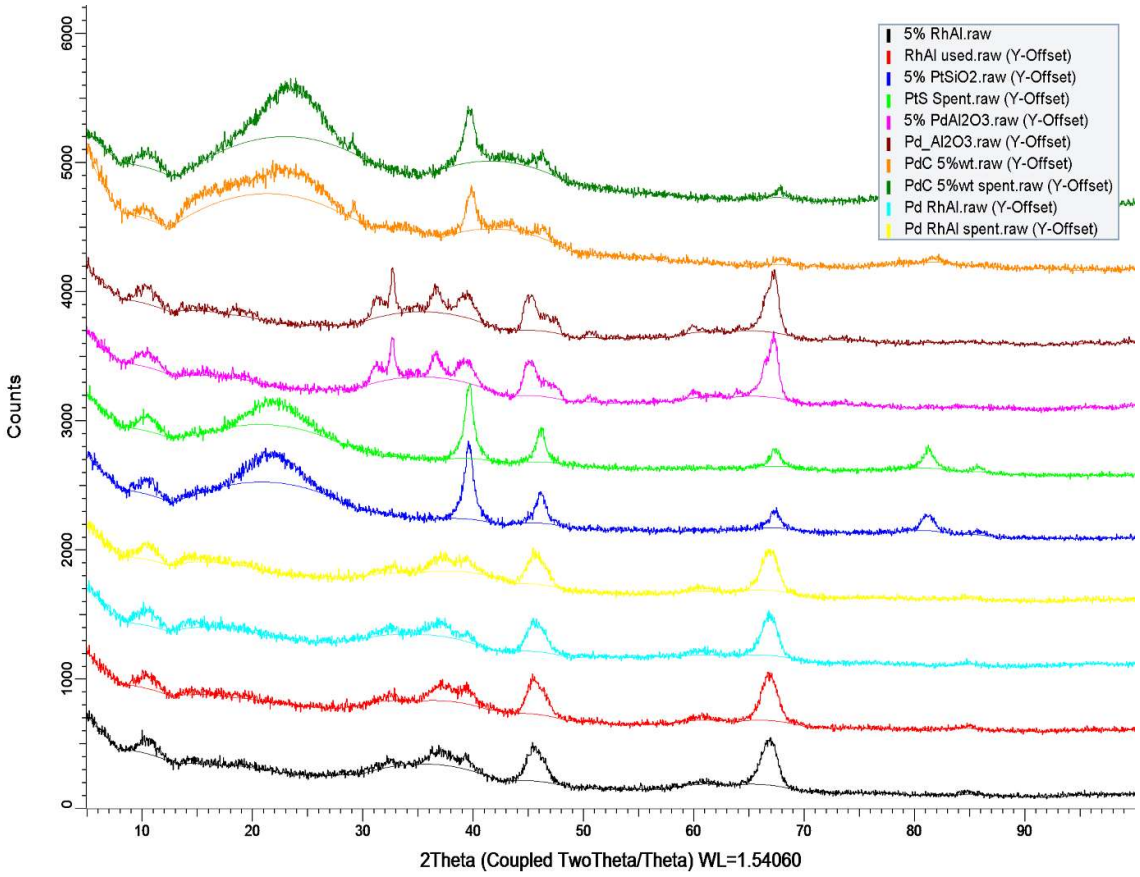
5% RhAl.raw
RhAl used.raw (Y-Offset)
5% PtSiO2.raw (Y-Offset)
PtS Spent.raw (Y-Offset)
5% PdAl2O3.raw (Y-Offset)
Pd_Al2O3.raw (Y-Offset)
PdC 5%wt.raw (Y-Offset)
PdC 5%wt spent.raw (Y-Offset)
Pd RhAl.raw (Y-Offset)
Pd RhAl spent.raw (Y-Offset)
Counts
0
1000
2000
3000
4000
5000
6000
10
20
30
40
50
60
70
80
90
2Theta (Coupled TwoTheta/Theta) WL=1.54060

Figure 3

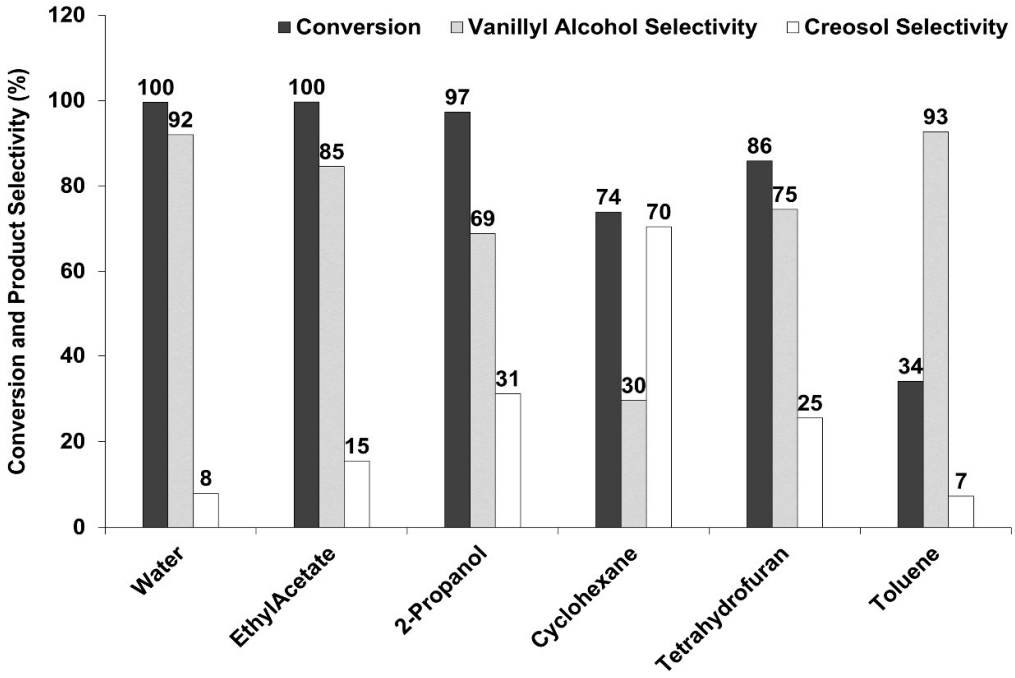
Conversion
Vanillyl Alcohol Selectivity
Creosol Selectivity
Conversion and Product Selectivity (%)
120
100
80
60
40
20
0
100
92
8
100
85
15
97
69
31
74
30
70
86
75
25
34
93
7
Water
EthylAcetate
2-Propanol
Cyclohexane
Tetrahydrofuran
Toluene

Figure 4

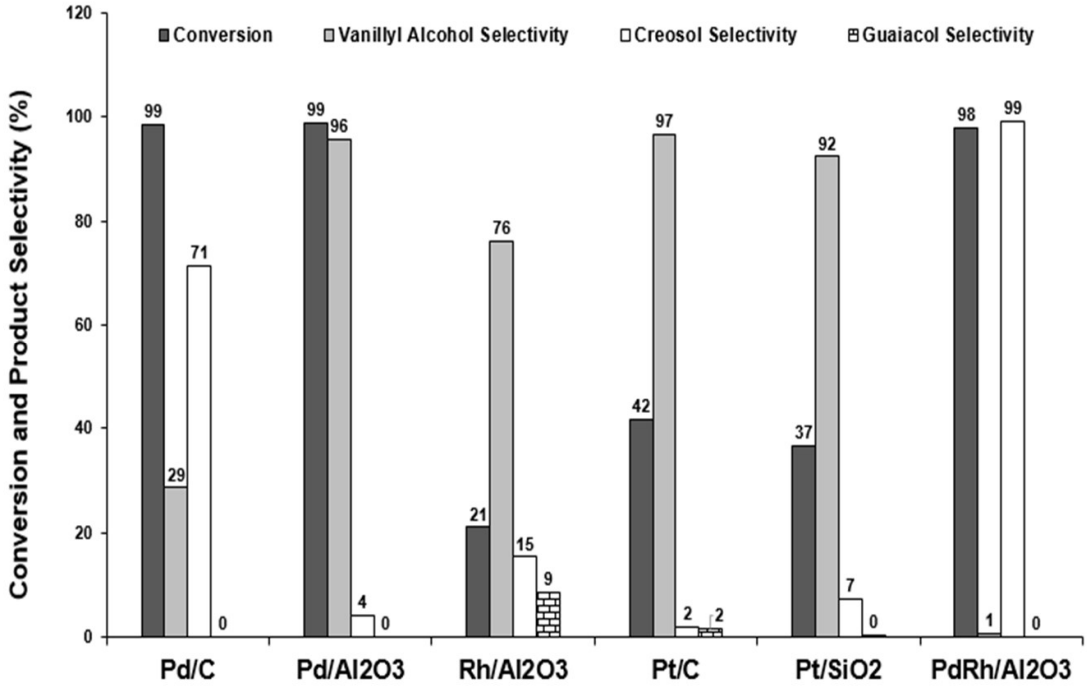
Conversion
Vanillyl Alcohol Selectivity
Creosol Selectivity
Guaiacol Selectivity
Conversion and Product Selectivity (%)
120
100
80
60
40
20
0
99
29
71
0
99
96
4
0
21
76
15
9
42
97
2
2
37
92
7
0
98
1
99
0
Pd/C
Pd/Al2O3
Rh/Al2O3
Pt/C
Pt/SiO2
PdRh/Al2O3

Figure 5

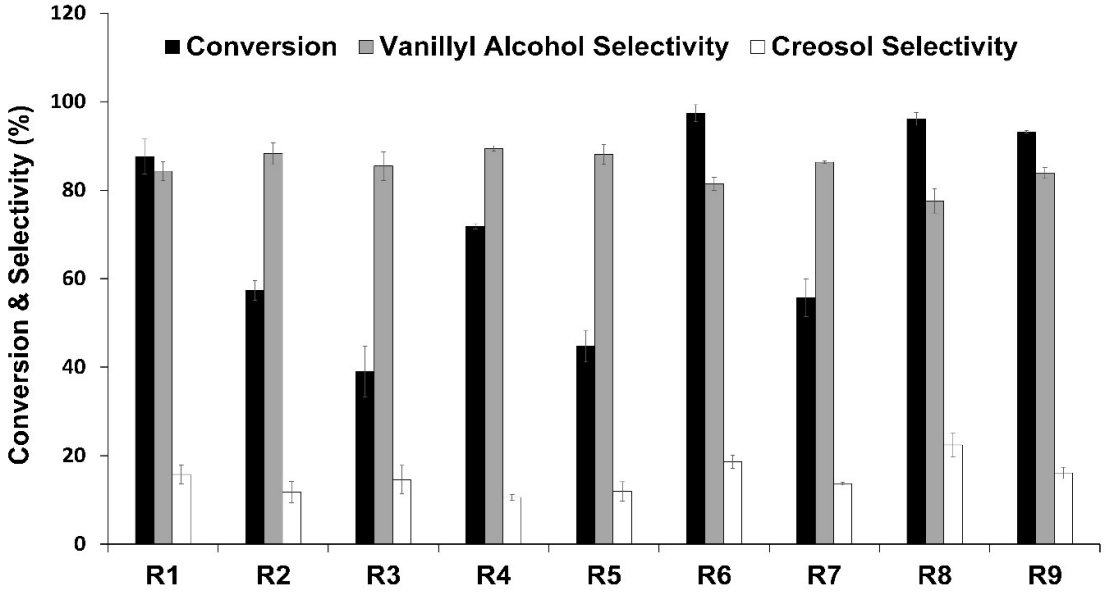
Conversion
Vanillyl Alcohol Selectivity
Creosol Selectivity
Conversion & Selectivity (%)
120
100
80
60
40
20
0
R1
R2
R3
R4
R5
R6
R7
R8
R9

Figure 6

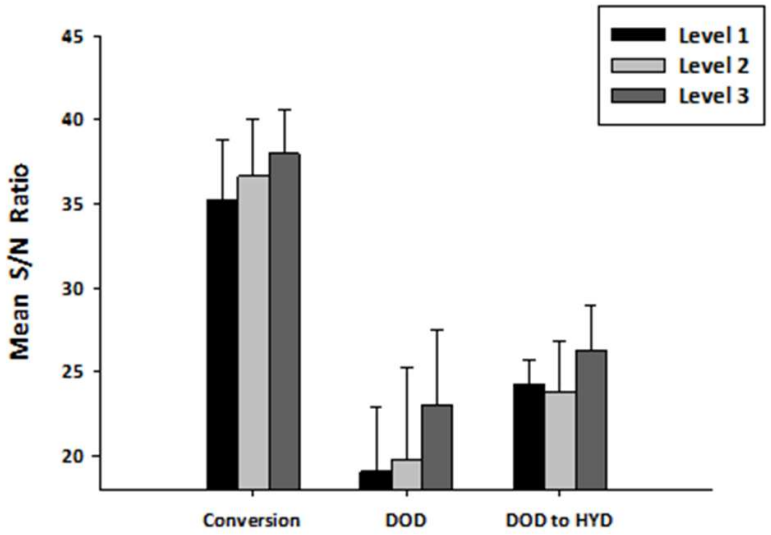
Level 1
Level 2
Level 3
Mean S/N Ratio
45
40
35
30
25
20
Conversion
DOD
DOD to HYD

Figure 7

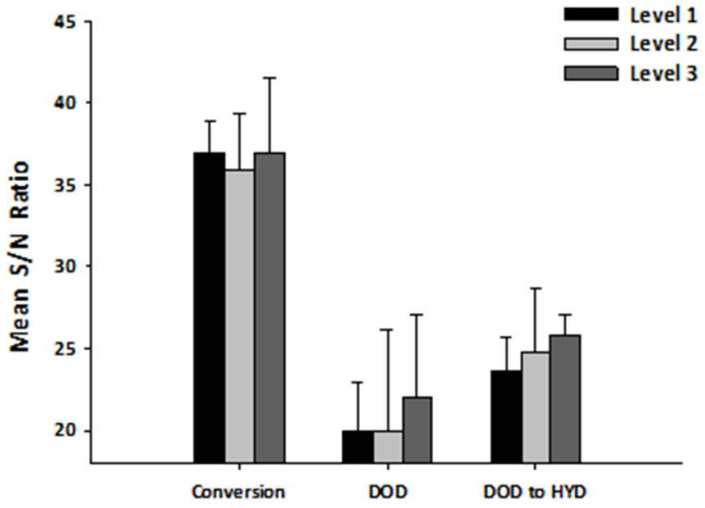
Level 1
Level 2
Level 3
Mean S/N Ratio
45
40
35
30
25
20
Conversion
DOD
DOD to HYD

Figure 8

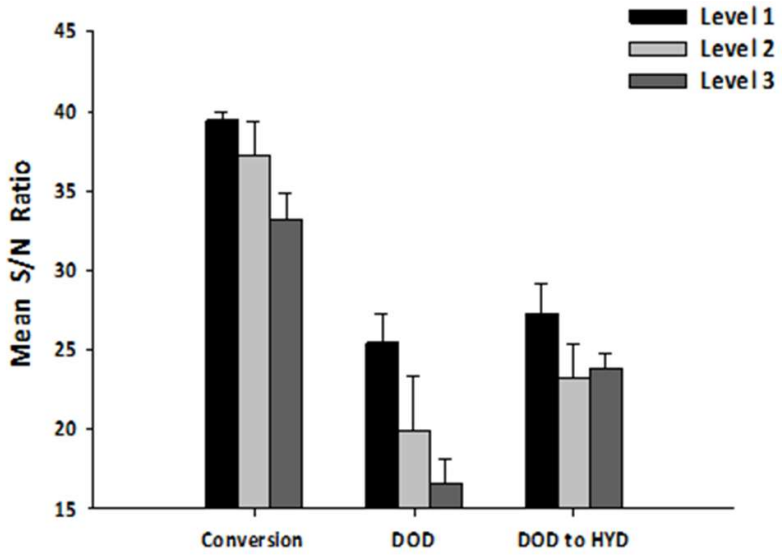
Level 1
Level 2
Level 3
Mean S/N Ratio
45
40
35
30
25
20
15
Conversion
DOD
DOD to HYD

Figure 9

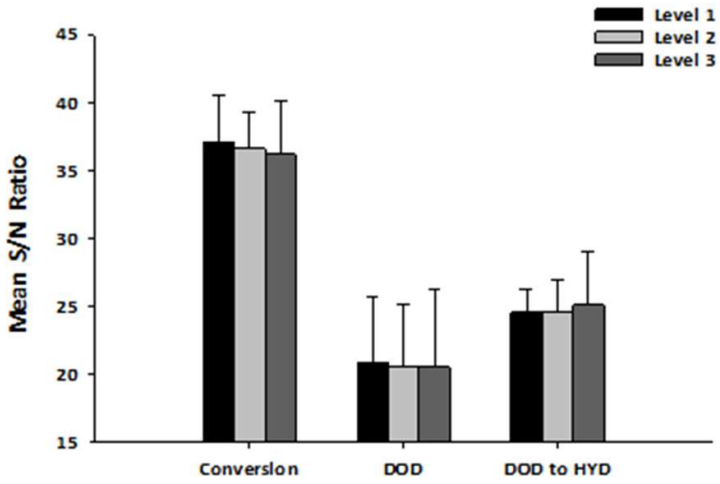
Level 1
Level 2
Level 3
Mean S/N Ratio
45
40
35
30
25
20
15
Conversion
DOD
DOD to HYD